Failure anticipation scheme in distribution systems based on wave distortions and Montecarlo methods

Bhandia, Rishabh; Chavez, Jose J.; Cvetković, Miloš; Garcia-Vite, Pedro M.; Popov, Marjan; Palensky, Peter

DOI
10.1016/j.ijepes.2023.109757

Publication date
2024

Document Version
Final published version

Published in
International Journal of Electrical Power & Energy Systems

Electrical Power and Energy Systems 156 (2024) 109757

Contents lists available at ScienceDirect

International Journal of Electrical Power and Energy Systems

journal homepage: www.elsevier.com/locate/ijepes

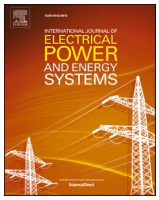

Review

Failure anticipation scheme in distribution systems based on wave distortions and Montecarlo methods

Rishabh Bhandia [a], Jose J. Chavez [a,b,*], Miloš Cvetković [a], Pedro M. García-Vite [c], Marjan Popov [a], Peter Palensky [a]

[a] Faculty of Electrical Engineering, Mathematics and Computer Science, Delft University of Technology, 2628 CD Delft, the Netherlands
[b] Tecnologico de Monterrey, School of Engineering and Sciences, Ave. Eugenio Garza Sada 2501, Monterrey, N.L. 6484, Mexico
[c] DEPI, Tecnológico Nacional de México Campus de Cd. Madero, Av. Primero de Mayo 1610, Los Mangos, 89460 Cd Madero, Tamps., Mexico

ARTICLE INFO

Keywords:
Incipient faults detection
Failure anticipation
Situational awareness
Signature analysis
Distribution systems

ABSTRACT

Anticipating failures is vital for maintaining a reliable power supply. Advanced measurement devices in the grid generate vast data that contains valuable information on grid operations. Initial signatures of an incipient failure are often reflected in this data in the form of electrical waveform distortions. Conventional protection schemes are not equipped to analyze these distortions and anticipate failures. There is a considerable research gap for a simple yet robust and universal failure anticipation and diagnosis scheme. This paper proposes a universal Failure Anticipation and Diagnosis Scheme (FADS) to detect incipient failures in AC distribution grids. The method comprises three short stages, helping the operator make an informed decision. In the first stage, the FADS scheme leverages the fundamental properties of electrical sinusoid waveforms to detect distortions. In the second stage, the distortion data is processed through pre-determined thresholds set in accordance with the system's regular operation. In the third stage, depending on the system, the FADS uses the extent of the violations of these thresholds and ranks the severity of the danger posed to grid operations. The classification helps determine if the waveform distortions are the signature of an incipient failure. The proposed FADS method's reliability, robustness and effectiveness are evaluated in incipient failure conditions of field events modelled in real-time simulations on standardized IEEE distribution feeders. The FADS is a high-speed distortion detector, is quite sensitive, and the method has high selectivity because of its nature.

1. Introduction

Today's world can be visualized as a highly digitalized, closely interconnected, and heavily interdependent system. A reliable power supply would be crucial to maintaining such a system's operational efficiency. Interruption of the power supply for even a small duration can lead to significant negative consequences. As stated in [1], conventional distribution system protection schemes are reactive in nature and are designed to detect major faults after they have occurred. However, in some cases, the time taken to detect the fault is not fast enough, and substantial damage can happen to the power system, which would require considerable time and resources to fix. Hence, there is a need for new anticipative protection schemes or technologies to detect non-conventional failures and disturbances in time so that any threat to normal grid operations can be fixed.

Failure in a power system can be described as any unplanned event that can disrupt grid operations. Hence, failures can be conventional failures (like line-to-ground faults) or non-conventional failures (like slow and progressive equipment damage, weather-related outages, and the cascading effect of other external events). Several different phenomena or disturbances can fall under the non-conventional failure category. These phenomena or disturbances do not usually leave a specific signature or trace (like overcurrent), which can be leveraged to detect them. Commercial protection relays successfully detect conventional faults, which have been standardized over time. However, there is a considerable research gap in detecting non-conventional failures.

Technological advancements have led to the creation of smart devices collectively known as Intelligent Electrical Devices (IED) that can provide high-resolution grid data. This data helps in efficient condition monitoring of the power system. Condition monitoring can be described

* Corresponding author.
E-mail addresses: rbhandia@ieee.org (R. Bhandia), j.j.chavezmuro@tec.mx, j.j.chavezmuro@tudelft.nl (J.J. Chavez), M.Cvetkovic@tudelft.nl (M. Cvetković), pedro.gv@cdmadero.tecnm.mx (P.M. García-Vite), M.Popov@tudelft.nl (M. Popov), palensky@ieee.org (P. Palensky).

https://doi.org/10.1016/j.ijepes.2023.109757
Received 1 April 2023; Received in revised form 6 November 2023; Accepted 28 December 2023
Available online 13 January 2024

as monitoring and identifying changes in different parameters of power system components [2]. Efficient condition monitoring will lead to enhanced situational awareness of the grid operations. This awareness would be essential to analyze waveform distortions as the signature of non-conventional failures and anticipate the incipient failure before it cascades into a blackout or an outage.

There have been few studies to design algorithms to detect non-conventional failures. The detection methods generally confine their analysis to similar failures grouped according to specific properties or behavioral patterns. These non-conventional failure patterns are often classified as power quality disturbances in the literature. In [3], the IEEE working group on Power Quality (PQ) Data Analytics describes power disturbances as persistent deviation from sinusoidal voltage or current waveforms. The report attempts to classify these power disturbances as one of the seven PQ disturbance categories. However, as mentioned in [4], incipient power system failures would not always manifest as a specific PQ disturbance. In [5], incipient faults in underground cables have been detected using similarity functions with high speed and accuracy. Incipient failure in insulators using high-frequency signal activities data has been analyzed in [6], while the Kalman filter-based method for incipient fault detection has been employed [7]. Online cable condition monitoring is used in [8] for fast detection of sub-synchronous resonance. Significant work has been done in [9] to develop a generic waveform abnormality detection method based on Kullback-Leibler divergence (KLD) to identify any equipment failure. In [10], specific feature extraction using smart meter signals has been used to classify power disturbances. Incipient failure detection has been performed using numerical modelling of fault patterns [11]. Weather-related failures have been analyzed, and detection methods are proposed in [12,13]. A comprehensive, holistic-level study has been conducted in [2] to classify incipient transmission network faults using various feature extraction techniques. The research work documented in [14] has contributed significantly to the field of anticipating failures in distribution networks. This innovation led to the development of the Distribution Fault Anticipator (DFA) tool. The results have been documented in [1,15]. The DFA tool relies on cross-referencing massive databases of fault and failure conditions recorded over the years to identify an incipient failure.

The non-conventional failures originating due to a similar cause need not always necessarily adhere to a specific pattern. The behavioral patterns of these failures can be random and highly unpredictable. Such a level of randomness needs a detection technique that leverages more fundamental aspects of the incipient non-conventional failure. As discussed in [15], when an incipient failure transforms into a full-fledged failure is referred to as the pre-failure period. The pre-failure period can last from seconds to months, making it preferable to have a fast detection technique so that the incipient failure can be detected and mitigated before causing any damage. The existing literature addresses the issue of incipient failures with varying degrees of success. However, they are restricted in their widespread application. Some techniques focus only on specific use cases like equipment failures; some can detect only certain kinds of disturbances like PQ disturbances or weather-related effects. Finally, some need to refer to the historical fault database. In [2,3,4], it is acknowledged that there needs to be a comprehensive and holistic, yet fast and easy to implement, failure anticipation technique. In [16] fault prediction methods are catalogued in two with respect to the available data. First, by using forecast and characteristics of the system data and second, by using labelled periodic recorded electrical signals. In addition, conventional faults are those that can be predicted using recorded data of the network, and non-conventional faults are related to weather conditions and human abruptions that cannot be predicted. Thus, the proposed method is limited to conventional faults not detected and/or located by classical protection schemes using labelled data This paper contributes to this field by proposing a Failure Anticipation and Diagnosis Scheme (FADS).

The rest of the paper is organized as follows: Section 2 describes the proposed failure anticipation and diagnosis scheme in detail. The section is split into different stages. In the first stage, a distorted waveform is differentiated from a typical sinusoid waveform by leveraging the fundamental properties of an AC current–voltage sinusoid waveform. In the second stage, the information from the first stage is processed through different indicators and threshold violations to determine if the distortions in the waveform are from a nonconventional incipient failure or everyday grid occurrences like switching or phenomena like noise etc. Section 3 discusses the application of the proposed method in two distribution feeders, the IEEE 39 nodes and the IEEE 13 node feeder, during underground cable failure and capacitor bank malfunctioning, respectively. The results highlight the accuracy and efficiency of the proposed method. The conclusion and discussions are presented in Section 4.

2. Failure anticipation and diagnosis scheme (FADS)

FADS is a data analytics-based approach that starts with acquiring raw data from grid measurements and ends with extracting useful information to anticipate non-conventional failures. FADS is implemented in three stages. An overview of the FADS can be seen in Fig. 1.

2.1. Stage I

This stage deals with raw data acquisition and detection of distortion in waveforms. It is meant to be implemented in the IEDs to distribute the data processing load at different places.

2.1.1. Raw data acquisition

The raw data required by FADS are time-stamped sampled voltage and current waveforms that can be collected from the existing IEDs monitoring the distribution grid in real-time. High-resolution raw data is desired for higher accuracy, but the sampling rate value does not impede FADS application. The proposed FADS do not need to have a fully observable system. Nevertheless, the grid must contain more than one IED element at different places to have information at different nodes.

2.1.2. Waveform distortion detection

The underlying concept behind the FADS scheme is that in ideal grid operating conditions in an AC distribution system, the electrical waveforms would always be sinusoidal. Any event affecting the grid operations would lead to intermittent or persistent deviation from the sinusoidal nature of the electrical waveforms. These deviations are collectively referred to as 'distortions' in FADS terminology. These distortions can be in the form of a PQ disturbance, a combination of different PQ disturbances or any other unexplained behavior or pattern. Irrespective of the form or pattern, it invariably leads to waveform distortions. Hence, distortions are considered the first signatures of an

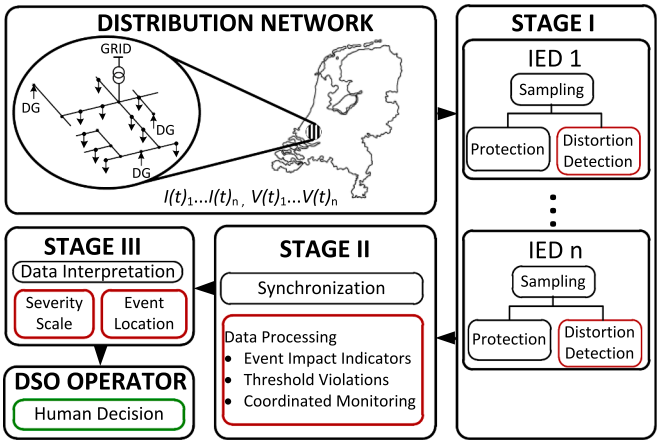

Fig. 1. Failure Anticipation and Diagnosis Scheme (FADS).

event affecting grid operations. However, electrical signals from real distribution systems are always distorted due to the variety of nonlinear elements and electronic devices connected to the grid. The voltage waveforms are usually more difficult to distort than current waveforms. This is particularly valid in voltage waveforms of substation buses. Hence, distortions in the voltage waveforms are more solid and reliable signatures of non-conventional failures. However, some buses are very weak in every grid, and in such a case, distortions due to intermittent earth faults and high impedance faults might also be reflected in the voltage waveforms. Therefore, the FADS is flexible in considering any bus voltage in the system and including current waveforms for analysis of the size constraints.

The maximum total harmonic distortion allowed (THDSE) by the Standard STD 519 is 5 % of the fundamental signal [17]. In this work, the system data is collected from the IEDs deployed in the system. All IEDs pre-process the electrical signals by an analogue low-pass filter to remove noise. Then the resulting signal is discretized by N samples per cycle. Then, an IIR filter based on the three-point cosine is used [18,19].

2.1.3. Waveform distortion detection

The next step is to differentiate between distorted waveforms and ideal sinusoids. Ideal sinusoids can be mathematically represented as complex exponentials. As seen in (1), Euler's formula represents a complex exponential as a sum of two trigonometric functions.

$$e^{j\omega t} = \cos\omega t + j\sin\omega t \tag{1}$$

where ω is the angular frequency (rad/s), t is time (s) and j is the imaginary unit. The authors used this mathematical formulation previously to detect High Impedance Faults (HIF) in [16].

Complex exponentials have certain unique properties. Firstly, the value of the function does not increase or decrease linearly with respect to time. Instead, the rate of increase or decrease is directly proportional to the value of the function at that instant. Secondly, complex exponentials are not infinitely increasing or decreasing. A complex exponential rotates around the unit circle in a complex plane. It starts to move from zero to peak value and from peak, back to zero and so on.

The violation of the unique properties would indicate that the waveform is not sinusoidal at that instant and would be detected as a distortion. The mathematical formulation of how FADS leverages the violation of these unique properties to see a distortion is explained next.

Consider a pure sinusoid signal uniformed sampled $f[k]$ as shown in Fig. 2. Assuming that the signal is a sinusoidal wave of period T, discretized by N samples per cycle, the samples can be denoted as: $(n\cdots k-1, k, k+1\cdots n+N)$. The samples are equally spaced in time at an interval of length (h), such that.

$$T = h \bullet N \tag{2}$$

Hence, the time instants of the samples collected can be denoted as: $(t_n\cdots(t_k-h), t_k, (t_k+h), \cdots, t_{n+N})$. As per (1), the sinusoid of samples $(k-1, k, k+1)$ at the time instants of $(t_k-h), t\_k, (t_k+h)$ can be mathematically represented as $(e^{j\omega(t_k-h)}, e^{j\omega(t_k)}, e^{j\omega(t_k+h)})$ respectively. Considering $g[k]$ as the difference of the sampled values for samples at k and $k+1$, it can be written in the interval $\{0, T/4\}$:

$$g[k] = \mathrm{Re}\left(e^{j\omega(t_k+h)} - e^{j\omega(t_k)}\right) \tag{3}$$

Simplifying (3):

$$g[k] = \mathrm{Re}(e^{j\omega t_k}\left(e^{j\omega h} - 1\right)) \tag{4}$$

Substituting $e^{j\omega t_k}\left(e^{j\omega h} - 1\right)$ as A:

$$g[k] = \mathrm{Re}(A) \tag{5}$$

Similarly, it can be written:

$$g[k-1] = \mathrm{Re}(e^{j\omega(t_k)} - e^{j\omega(t_k-h)}). \tag{6}$$

Simplifying (6):

$$g[k-1] = \mathrm{Re}\left(\frac{e^{j\omega t_k}\left(e^{j\omega h} - 1\right)}{e^{j\omega h}}\right) \tag{7}$$

or:

$$g[k-1] = \mathrm{Re}\left(\frac{A}{e^{j\omega h}}\right) \tag{8}$$

Since $e^{j\omega h}$ is a complex exponential, it will rotate around the unit circle and the value would be in the range $\{-1, 1\}$. In the interval of $\{0, T/4\}$, the maximum value would be one, indicating a positive peak and the sinusoid will then return to zero at $T/2$. If zero is taken as starting reference, the real value of $e^{j\omega h}$ would be less than one until it reaches the peak. Hence, the value of $g[k-1]$ in (8) would be greater than $g[k]$ in (5) in the interval $\{0, T/4\}$. Similarly, the phenomenon will reverse in the other half cycle. Summarizing, for any pure sinusoid for a cycle of period T:

$$g[k-1] > g[k],\ k \in \left\{n, n+\frac{T}{4}\right\} \bigcup \left\{n+\frac{T}{2}, n+\frac{3T}{4}\right\} \tag{9}$$

$$g[k-1] < g[k], k \in \left\{n+\frac{T}{4}, n+\frac{T}{2}\right\} \bigcup \left\{n+\frac{3T}{4}, n+T\right\} \tag{10}$$

The violation of (9) or (10) will constitute a distortion.

2.1.4. Implementation

Real-time monitoring of electrical waveforms by IEDs is necessary for enhanced situational awareness of grid operating conditions. However, real-time monitoring leads to massive data generation. Some amount of pre-processing is required at the device level before the data can be synchronized for further classification. Hence, FADS proposes to implement distortion detection functionality in the existing IEDs in parallel to their traditional protection functions as seen in Fig. 1. The low computational burden and minimal memory requirements of (9) and (10) make its implementation feasible. The distortion detection reporting is stored in a tuple (d, t) where d indicates the occurrence of the distortion at time t. It can define $d = 1$ if distortion is detected and $d = 0$, if distortion is not detected. The distortions detected need to be stored in temporary datasets of small time frames of a specified length, to perform synchronization and extract meaningful information before moving to analyze the next set of distortions. The time frames of these datasets are user dependent. If it has r IEDs such that $r = 1, 2, 3\cdots N$, then the dataset Sr in the time interval of (a_r, b_r) can be represented as:

$$S_r = \{(d_f, t_f) | d_f \in \{0, 1\}, t_f \in (a_r, b_r), f = (1, 2, 3, \cdots N)\} \tag{11}$$

The dataset Sr from each IED containing information of the occurrences of distortions is the final output of Stage I and the input to Stage II.

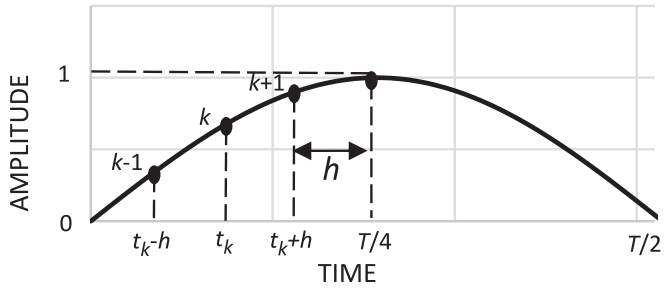

Fig. 2. Pure sinusoid sampled signal f[k].

2.2. Stage II

In this stage, the data processing helps evaluate and classify the event's severity. Common distribution grid events like load switching

and feeder energisation are non-harmful pre-planned events that still produce distortions for a few instances. Hence, Stage II comprises the steps to differentiate between a harmful and a non-harmful event.

2.2.1. Synchronization

Synchronized measurements are necessary for data analytics to extract useful information to analyze the operating condition of the grid. Thus, the time-stamped datasets from all the IEDs must be synchronized. The distortions detected in the time frame t_f of each dataset for each IED are summed up in (12). This information forms the core of data processing.

$$C_r = \sum_{p=1}^{|S_r|} d_p \tag{12}$$

2.2.2. Data processing: event assessment

The first step after collection and synchronization of the data is to identify the nature of the event causing waveform distortions. An accurate assessment of the event causing distortions can help us to determine the extent of disruption can cause to normal grid operations. A planned event like load switching generally produces few distortions resulting in a new normal steady state that persists over time. Weather effects, degrading equipment, etc., often produce multiple distortions over time which are more limited in their duration and do not sustain in the sense of being long-term steady-state changes.

The key is determining the thresholds for distortions to be detected in a certain period over which the distortion inducing event can be classified as harmful or not.

- Time-Period: The distortions recorded would be compared against the thresholds to check if they are violated in this minimum time interval. The value is user-dependent and can be changed depending on the grid operator's requirements.
- Threshold Violation: In FADS, the violation of thresholds is used as the first classification to determine whether the event is harmful or not. Monte Carlo trials are used to determine the thresholds. The test systems used are the long and lightly loaded IEEE-34 and the IEEE-13 Node Feeders [20]. The test systems have specific measurement points where the voltage/current waveforms are monitored, and distortions recorded (see Fig. 3).

In this paper, common grid events, namely load switching and capacitor switching, are simulated at different locations in the distribution grid. These grid events produce distortion in the waveforms. However, unlike those emanating from an incipient failure, the distortions produced will not usually be sustained over time. Monte Carlo trials, a comprehensive stochastic process [21], are used to consider all random eventualities of waveform distortions to determine thresholds accurately. The Monte-Carlo variables, listed in TABLE I, are the connection of two and three phases loads in 9 different places for IEEE 34 nodes and 4 different places for IEEE 13 nodes. Also, as a variable, capacitor banks type Y, Δ, and Δ g are connected at several different points in the systems.

2.2.3. Data processing: coordinated monitoring

The concept of coordinated monitoring is crucial for the proposed method. The waveform would have a high probability of being non-uniform across the grid. Hence, the measurement points close to the incipient failure location will pick up higher distortions than those far from the location. If the incipient failure is affecting a certain section of the grid, there should be enough observability to conduct operations in that section instead of affecting the entire grid. On the other hand, it is also important to know if the incipient failure has begun to affect other sections creating a cascade effect. This dilemma can be resolved by coordinated monitoring and smart analysis of the distortion data from different measurement points. In the study cases and selected measurement points, the closer the measurements are to incipient fault locations, the larger the distortions recorded. However, this may be different in other scenarios. Therefore, the method cannot be taken as a fault locator. This topic is outside the scope of this document. In addition, the recording point localization is not studied in this paper, but a point in each lateral may increase the accuracy of the method.

Coordinated monitoring comprises two different levels of monitoring. The lower level is the Local Measurement Device (LMD) level to gauge the intensity of the event affecting the grid operations at the place of measurement. The higher level is the Distribution System (DS) level (comprising analysis of distortion data from all the measurement devices present in the grid) to gauge the impact of the event. The LMD level monitoring depends on the distortions the standalone measurement device recorded at that point. However, the concept of Common Reporting is introduced for the DS level monitoring. The time-stamped synchronized dataset can be analyzed to observe how many

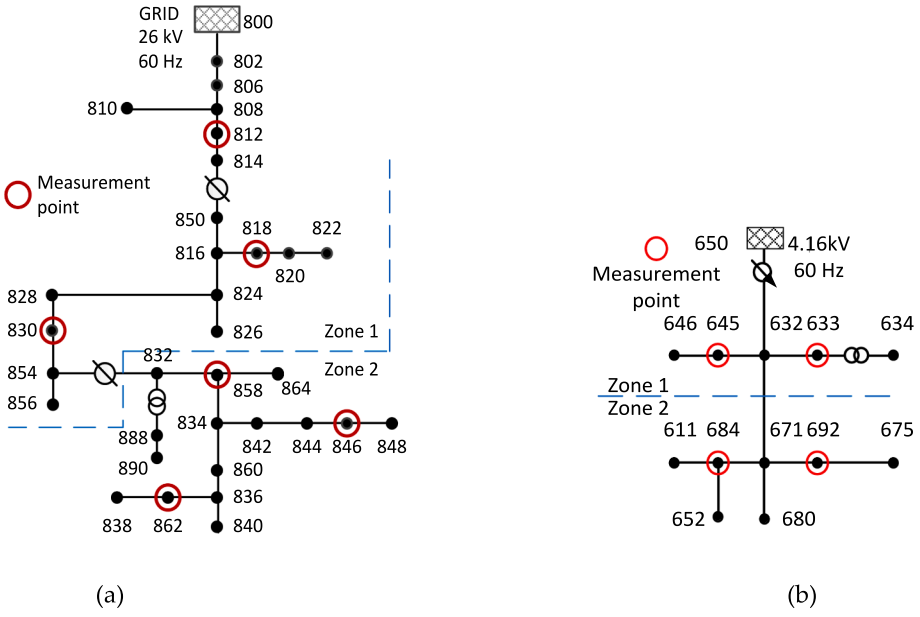

Fig. 3. Node Feeders for the simulation cases with measurement points, (a) IEEE-34 node feeder, and (b) IEEE-13 node feeder.

measurement devices in the grid record distortions simultaneously. Common Reporting helps estimate how evenly the incipient failure affects the entire grid operations across the network. This information further assists the user in planning the response strategies accordingly.

However, there is an obvious disadvantage attached to the DS level monitoring. Some measurement points at certain sections might report zero distortions for a large distribution grid such as the IEEE-34 node feeder. This will lead to an overall zero common reporting, which will mislead the DSO operator to assume that the grid is unaffected. Hence, the concept of Grid Zoning is introduced to refine the DS level monitoring further. Grid Zoning aims to divide the network into multiple observation zones providing better situational awareness of the grid. It will depend on common reporting of distortions recorded by measurement points installed in that zone.

To summarize, coordinated monitoring entails:

- LMD Level Monitoring: Distortion recorded at the local device at a particular measurement point.
- DS Level Monitoring: Common Reporting is the number of distortions recorded by each measurement point in the grid simultaneously. This monitoring level is further subdivided into grid zoning.
- DS Grid Zone Level Monitoring: Common Reporting of distortions recorded by all measurement points in the defined grid zone.

The concept of coordinated monitoring is not to choose between either LMD or DS Grid Zone level monitoring but rather utilize the complementary effect of both monitoring strategies for better grid observability and enhance situational awareness.

2.2.4. Data Processing: Monte Carlo trials

- Setup: The measurement points in the test systems are seen in Fig. 3. The data window for the dataset recording the waveform is kept at 0.1 s (also called reporting interval). It implies that after every 0.1 s, the existing dataset would move to Stage II, and a new dataset would be simultaneously created in Stage I to record waveform distortions, and the process will continue.

The system is divided if necessary. This work divides the IEEE-34 and the IEEE-13 distribution systems into two grid zones. The zoning is done such that both zones have equal measurement devices. Optimal grid zoning would also require further studies and tests, which is outside the scope of this paper. Grid zone 1 consists of areas covered by the measurement devices at nodes 812, 818, and 830 in IEEE-34, and 645 and 633 in IEEE-13. Grid zone 2 consists of areas covered by measurement devices at nodes 846, 858, and 862 in IEEE-34 and 684 and 692 in IEEE-13.

- Execution: The voltage waveforms are used in this work for FADS analysis because they are more resilient to distortions than current waveforms. Hence, only events genuinely threatening grid operations would produce noticeable distortions in voltage. The waveforms are sampled 128 times per cycle, which leads to a reasonable combination of high-resolution and computing power requirements. Distortions recorded are summed and represented as a percentage of samples distorted to the total number of samples in each dataset containing distortion instances information for the reporting interval of 0.1 s. The size of the reporting interval is essential to detect incipient faults using this method. Although the detection distortion method used in Stage I is fast and only needs fourth samples to detect a disturbance in Stage I, the window for the reporting time may be 0.1 or greater depending on the available resources. With this size of windows, the method can be used without making substantial changes in thresholds. This is not the case for reporting intervals smaller than 0.1 s in those cases, incipient faults may not be detected in all windows and a new threshold must be found.

The calculation of the threshold at both levels is done for each Monte-Carlo trial for every switching event at both systems seen in Fig. 3. In total, 3900 trials are done and summarized in Table 1. The LMD level threshold concerns the threshold at the local measurement device. Data from any measurement point cannot be taken as a reference point since it will bias the calculation of the threshold. The measurement point records the highest percentage of distortions for each event and is used for the LMD threshold (13). An average percentage of distortions is then calculated for that event, utilizing the total percentage value of the highest recorded distortions and the number of Monte-Carlo trials conducted to determine the LMD level thresholds as in (14).

$$LMD^{k}_{threshold} = \max(\%distortions_{all\ \ events}) \tag{13}$$

Where k is the kth local measurement device.

The DS level-Grid Zone threshold (DSthreshold) concerns the threshold determination of the different grid zones. Thus, this paper notes the common reporting of distortions recorded across all the measurement devices for each switching event of both zones. The percentage is obtained and the final average percentage value for the threshold of each grid zone of DS level is determined. In addition to covering any other uncertainty, a safety margin of 10 % is added (14).

$$DS_{threshold} = \frac{1.1}{N}\left[\sum\nolimits_{k=1}^{N} LMD^{k}_{threshold}\right] \tag{14}$$

N is the total number of measurement points.

As seen in Fig. 4 (a), the Monte-Carlo trials conducted for the IEEE-34 and IEEE-13 systems give the LMD threshold values for load and capacitor switching as 2.7 % − 6.5 % and 2.1 % −4.8 %, respectively. Similarly, in Fig. 4 (b), one can observe the DS-grid zone level threshold values. The values for load switching are 1.5 % and 1.6 % at zone 1 and 2, respectively. The values for capacitor switching are 4.2 % and 4.6 % for Zone 1 and Zone 2. Similar results are obtained for the IEEE-13 system case. A flowchart of the Monte Carlo trials is provided in Fig. 5.

Only capacitor banks and load switching are analysed in this paper. There are other types of distortions during normal operation, such as transformer energisation, motor starting, reconfiguration, etc. This paper does not cover those events due to the extensive simulations needed. However, considering those events in the limit calculations may result in a comprehensive threshold.

2.3. Stage III

This stage provides metrics to interpret the incoming data from Stage II. The metrics help to determine the severity of the event. It is only sometimes enough to differentiate between events as harmful and non-harmful. A harmful event could be anything ranging from localized disturbance to a large-scale blackout affecting entire grid operations. A very harmful and severe event will cause numerous and sustained waveform distortions reflected throughout the grid. A relatively less

Table 1
Monte-Carlo trials overview.

Load Switching					
IEEE-34			**IEEE-13**		
Type	Positions	Trials	Positions	Trials	Total
2-ϕ	9	60	4	60	780
3-ϕ	9	60	4	60	780
Capacitor Switching					
IEEE-34			**IEEE-13**		
Type	**Positions**	**Trials**	**Positions**	**Trials**	**Total**
Y	9	60	4	60	780
Δ	9	60	4	60	780
Y-ground	9	60	4	60	780

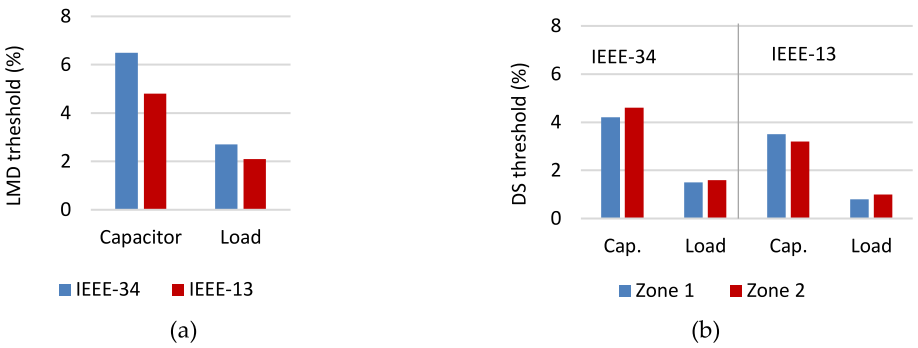

Fig. 4. Average percentage distortion, Monte-Carlo trials: (a) LMD threshold determination and (b) DS-Grid Zone threshold determination.

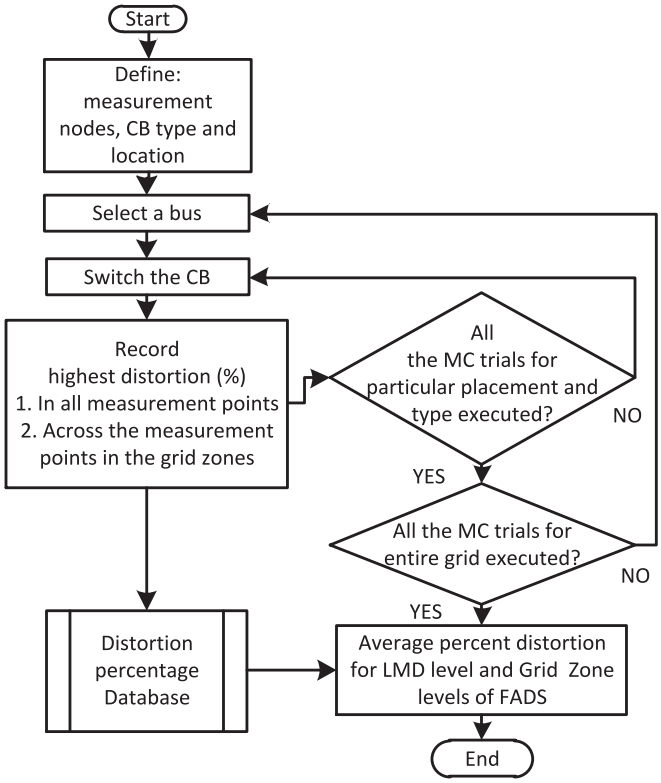

Fig. 5. Flowchart to obtain LMD and grid zone levels by Monte Carlo procedure.

severe event will cause fewer and localized waveform distortions. It is never good to interrupt the supply to the entire grid to fix comparatively less harmful localized grid events. The planning of the response actions also depends on how severe the event is. A zero severity rating (SR) indicates normal grid operation with no intervention needed. Although capacitor switching is a relatively harmless event, it causes more distortions due to the harmonics produced. Usually, it will not lead to any harmful effects.

However, to be extra-cautious and have sufficient time to prepare for a cascading effect, the percentage distortions of the capacitor rating have been rated on the SR scale. An SR level would indicate normal grid operations with minimal risks but, at the same time, would also indicate exercising caution by being on alert. Such a cautionary approach will help to keep a check for change to higher SR levels. In the Monte-Carlo trials, the difference in percentage samples distorted in each reporting interval between load switching and capacitor switching events is around 3 % to 4 %. Hence, a 4 % buffer differentiates between the different LMD severity rating levels. The overall percentage of distortions for the Grid Zone level is less than LMD levels. Hence, a slightly reduced buffer of 3 % is used between the levels for Grid Zone SR. The buffers are used throughout to define further levels and associated actions. In the empirical studies conducted, it is found that generally, a single phase to a ground fault until 0.3 s. from the commencement of the fault had average percentage distortions in LMD levels ranging from 15 % to around 35 %. Hence, in the presented SR scale, keeping a margin of safety, anything beyond 11 % in LMD levels is considered a full-scale fault, and SR scale is not defined further than level 4. The SR scale is defined in Table 2, and the interpretations are provided in Table 3. The scale is valid as long as the sampling time remains constant and the reporting time is equal to 0.1 s or greater.

3. Simulation cases

The FADS performance evaluation is carried out on an RTDS- Matlab® co-simulation platform under different incipient failure scenarios. The test node feeders are developed in the Real-Time Simulation Software Package (RSCAD®). The IEDs elements are also implemented in RSCAD. The already filtered and discretized signal is sent outside RTDS by a GTNET card. The data is transferred using a local area network (LAN) transmission control protocol (TCP). The communication at this stage is unidirectional. Finally, the data is received on a PC with MATLAB ® software.

3.1. *Underground cable failure*

This case study reproduce the event of underground cable failure documented in [18] in the real time platform. The sequence of events is planned such that the progressive degradation of the malfunctioning cable is realistic to the one documented in [18]. The initial signatures are in terms of transients in voltage profiles, which lasted barely for 0.22 cycles. Since it is a sub-cycle transient, the conventional relays do not take action. Over ten months, 140 such sub-phase transients were recorded, ranging from 0.22 to 0.47 cycles.

3.1.1. *Experiment modeling*

A modified IEEE-13 node feeder is used for experimental modelling. At node 650, not only the ideal source (4.16 kV) is connected, in addition, two sources, 0.25 kV and 0.06 kV, with frequencies of 180 Hz and

Table 2
Severity rating scale.

SRL	Interpretation	Possible response
0	Normal Operation	No intervention needed
1	Minimal Risk, some usual grid operations	On alert, to keep checking for change in severity rating
2	Definite risk, unusual happenings	Plan adequate response and implement it
3	Major risk, fault occurrence imminent	Implement quickest response possible

Table 3
Severity rating interpretation.

LMD Level Rating Percentage of distorted samples in each reporting interval	Severity Rating	Number of distortion detected
< 4 % distorted samples	0	< 30
(4–8)% distorted samples	1	30 to 59
(8–12)% distorted samples	2	60 to 89
>12 % distorted samples	3	>89
DS-Grid Zone Level Rating		
< 3 % distorted samples	0	<70
(3–5)% distorted samples	1	70 to 115
(5–7)% distorted samples	2	116 to 161
> 7 % distorted samples	3	>162

420 Hz, respectively, and a white Gaussian noise generator are also connected. The resulting waveforms are corrupted mainly by the third and seventh harmonics and high-frequency components. The sampling frequency is 8 kHz, and the analogue filter is a low-pass filter cut-off frequency at 2.8 kHz, ±5%, 3 dB. The digital filter is a Full-cycle cosine.

The cable failure is simulated between nodes 675 and 692. For simplicity and considering the long period of an actual field event, the modelling of the degradation of the cable is divided into four stages, indicating the transition from a healthy state to a total cable breakdown at the end of the 10th month. The four stages are associated with a certain transient occurrence (Toc) and duration (TD) in terms of the waveform cycle, as seen in Table 4.

3.1.2. Simulation results

The simulation runs for 124 s. However, only the most representative signals are included in Fig. 6. Fig. 6(a-I) and Fig. 6 (a-II) show voltage in phase C. The signal is corrupted mainly by the 3rd, 7th, and other harmonics. Nevertheless, the method handles this distortion without modifications. In Fig. 6 (b), 6 (c), 6 (d), and 6 (d), the phase C voltages at the nodes highlighted in Fig. 3 (b) are shown during 0.8 s. These voltage signals are from different time intervals to see the cable failure evolution. First, Fig. 6 (b-I), and Fig. 6(c-I), the transients are rare and cannot be considered harmful. However, in Fig. 6 (e-I), the failure becomes more often and can be seen two transients in the same interval of time.

The concise summary of the simulation results can be seen in a graphical representation in Fig. 7. Due to the enormous amount of data, the SRs across different measurement points for each sequence phase are presented separately. Therefore, for event sequence Phase-1, 50 s implies 500 reporting intervals of 0.1 s for each measurement point. Even though the phase duration is 50 s, the transient appearance frequency of every 2 s leads to a few level 2 reporting, mainly restricted to nodes 684 and 692. Without level 3 reporting and with negligible level 2 reporting, in proportion to the simulation duration, no conclusions can be made regarding incipient failure during event sequence phase 1. In Phase-2, the duration is reduced to 37.5 s. There is no level 3 reporting. The level 1 and 2 reporting during Phase-2 stay approximately constant as per Phase-1, but the actual interpretation would be that there is a proportional increase in the reporting as the duration of Phase-2 is less than Phase-1. After observing Phase-1 and Phase-2 reporting, it can be construed that there is some indication of possible issues with the grid operations, and maintenance teams may be kept on standby. In Phase-3, the duration is reduced even more to 24 s, the first level 3 reporting is observed, and the level 2 reporting is proportionately higher. The grid zone result observations also indicate a possible event location in Zone 2. Phase-4 reports a proportionately higher number of level 3 and 2 SRs, mainly for Zone 2, confirming an incipient failure in Zone 2.

The end of sequence Phase-2 gives an inkling of a possible incipient failure, and by the end of Phase-3, the possibility of incipient failure gets stronger. The ideal approach is to act sometime during sequence Phase-3 or at the end of sequence Phase-2. Since the entire event stretched around ten months, FADS implementation results of the simulated case study suggest that FADS implementation could have helped the early detection of an underground cable incipient failure.

Table 4
Transient occurrence and its duration.

	(A) Underground Cable Failure		**(B)Capacitor bank switching Malfunction**	
Event Sequence	Transient occurrence (Toc) & duration (TD) in cycles	Simulation Time	Transient occurrence (Toc) in cycles	Simulation Time
Phase-1	Toc = 120, TD = 0.2	50 s	Toc = 60	120 s
Phase-2	Toc = 75, TD = 0.3	37.5 s	Toc = 30	90 s
Phase-3	Toc = 37.5, TD = 0.4	24 s	Toc = 15	50 s
Phase-4	Toc = 15, TD = 0.5	12.5 s	–	–

Toc is measured in cycles, every *n*th cycle the event takes place.

3.2. Capacitor bank malfunction

Capacitor banks are an important asset in the distribution feeder and are used to improve the power factor, provide voltage support, etc. A high-power factor ensures a high quality of the power supply and loss minimization. Hence, the correct operation and maintenance of capacitor banks are a priority. In this case study, the event data of the capacitor bank switch malfunction documented in [14] is used and attempts to reproduce it in the real-time platform.

The event sequence lasted 2½ months before the damaged equipment was located and replaced. Initially, the capacitor bank is successfully switched. However, after a while, the monitoring systems in substations detected some unexplained transients. The events do not cause any alarm in conventional protection schemes, including the state-of-the-art. In addition, Advanced Metering Infrastructure (AMI) did not raise any alert or suspicion. The frequency of transients increased over time to twenty-one instances per day, hinting at equipment damage accelerating towards failure. When the utility acted after 2½ months, around 500 instances of transients are recorded. The cause of the transients is found to be a malfunctioning switch that conducts current even after it is in open state, leading to internal damage to the capacitor bank.

3.2.1. Experiment modeling

This document uses the IEEE-34 node feeder to recreate the event. The capacitor bank is connected at node 854, and phase C is designed to malfunction. The capacitance is set to 1.9252 mF per phase, which is similar to the rating of capacitors connected in the IEEE-34 system. It is connected to the grid through a vacuum switch, which is modelled as ideal. During the close state, the switch is equal to 0.1 Ω and during the open state is equal to 1 M Ω. The phase C switch presents a resistance equal to 38.44 Ω in an open state, thus resulting in a path for the current flow through the switch [22]. The produced event gradually damages the equipment leading to eventual equipment failure.

3.2.2. Simulation results

The simulation runs for 260 s. Fig. 8 shows the phase C voltage waveforms for the measurement points highlighted in Fig. 3 (a). The waveform is not used since 818 is a single-phase measurement point (phase A). Zone 1 recordings are based on common reporting of nodes 812 and 830. The zoomed version of the voltage's waveform distortions is shown in Fig. 8 (a-II), (b-II), and (c-II) to spotlight the transient events.

A summary of FADS results and instances of SR at different measurement points and zones is presented in Fig. 9. In Phase 1, Fig. 9 (a), the transients appear every 1 s leading to a few instances of level 1 SR. Expectedly, the measurement point closest to the event records most instances. Even though there is a single instance of a level 2 rating, the observations are inconclusive to confirm the presence of incipient

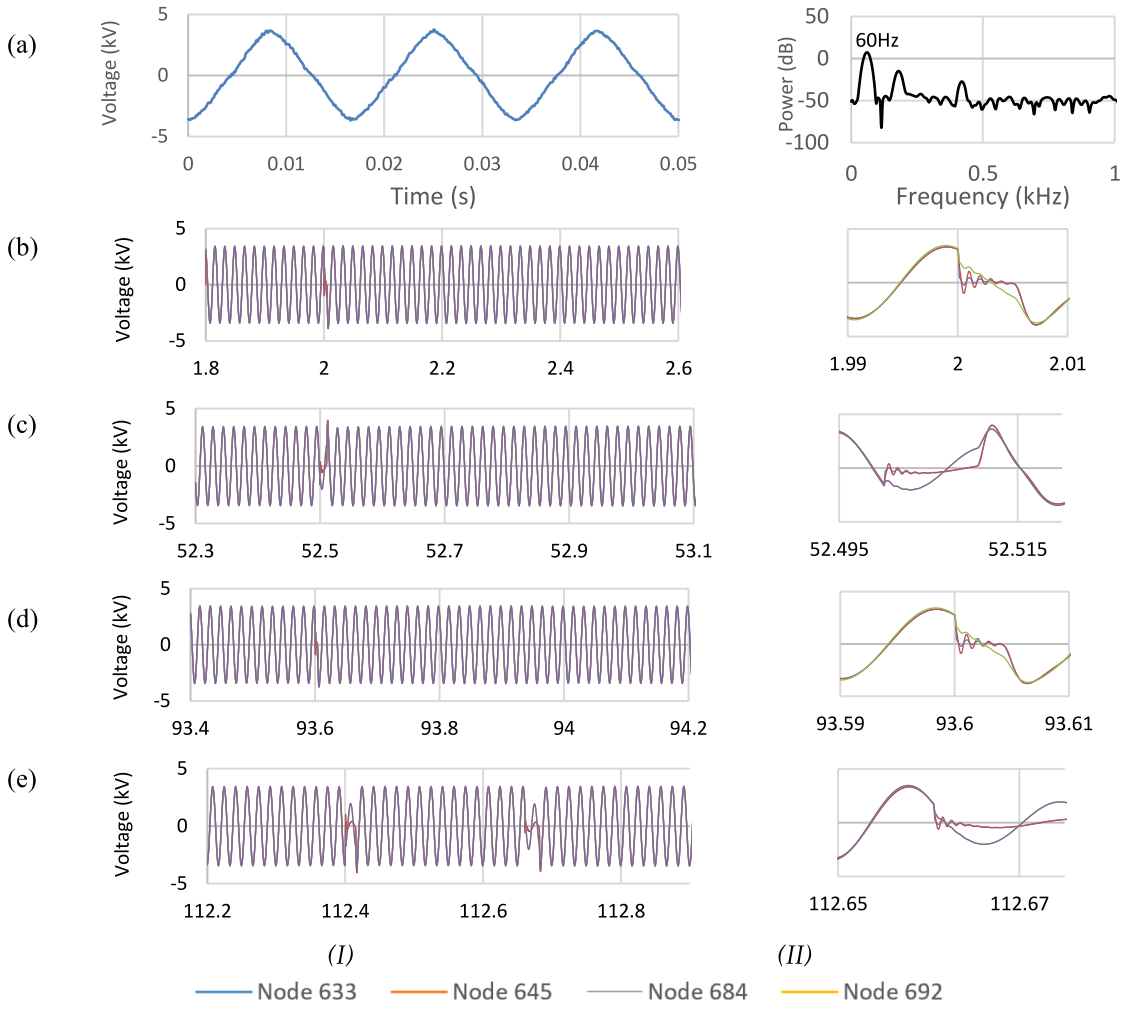

Fig. 6. Underground cable failure event sequence phases showing phase C voltage waveform at different measurement points. (a-I) raw voltage at bus 645, and (a-II) the total harmonic distortion in steady state conditions (b-I) event sequence phase-1 and a zoom (b-II), (c-I) event sequence Phase-2 and a zoom (c-II), (d-I) event sequence Phase-3 and a zoom (d-II), and (e-I) event sequence Phase-4 and a zoom (e-II).

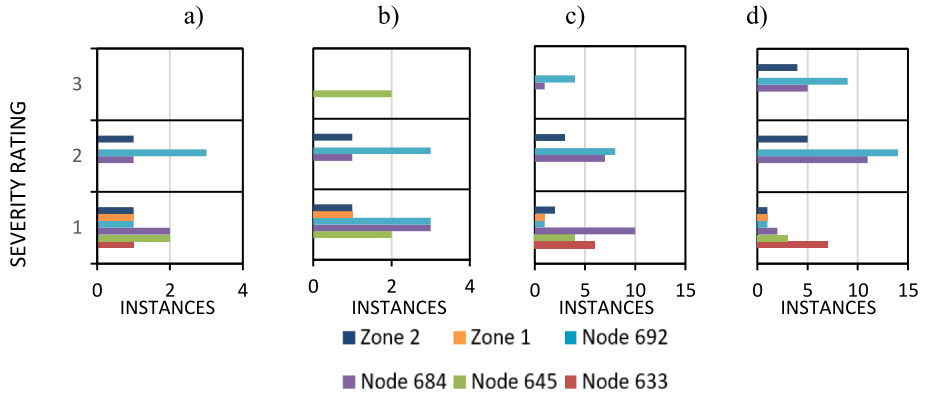

Fig. 7. Instances of different severity range (SR) at different measurement points for each event sequence phase during FADS implementation for Underground cable failure event. (a) Event sequence Phase-1, (b) event sequence Phase-2, (c) event sequence Phase-3, and (d) event sequence Phase-4.

failure. In Phase-2, Fig. 9 (b), the transients appear more often, and as a result, several instances of level 1 and level 2 ratings spread across different measurement points are observed. The first instance of level 3 reporting is also noticed. From Phase-2 observations, the presence of an incipient failure in the grid can be concluded. On the other hand, the Grid Zone SRs are inconclusive since instances of ratings of both zones are very similar, making it difficult to determine in which zone the maintenance teams should be dispatched. The LMD level ratings can be used to locate the event. Since the difference between instances of level 2 ratings for nodes 830 and 858 far outnumber other measurement points, the search area priority could be the segments between those nodes. In Phase-3, Fig. 9 (c), it becomes clearer that incipient failure is

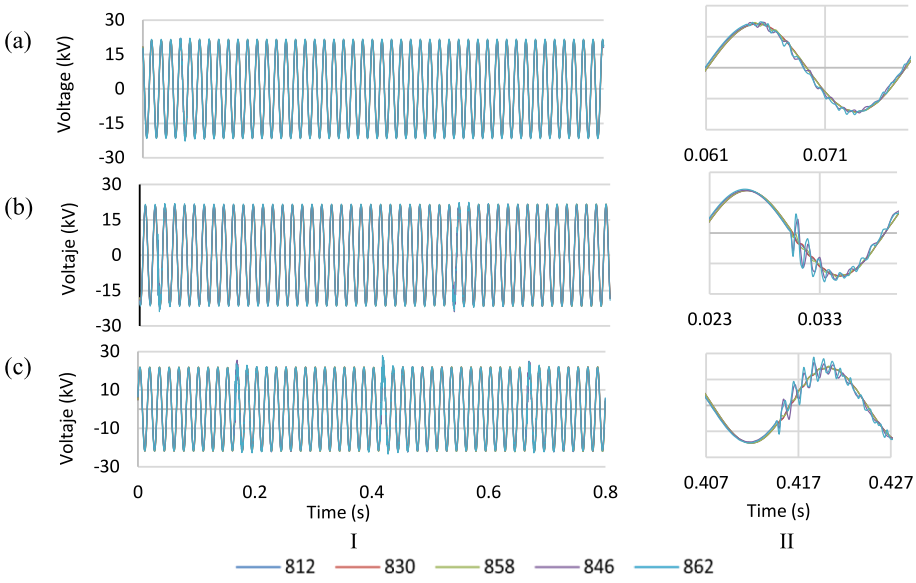

Fig. 8. Capacitor bank switch malfunction event sequence phases showing voltage waveform distortions for different measurement points (Phase C). (a-I) event sequence phase-1 and a zoom (a-II), (b-I) event sequence phase-2 and a zoom (b-II), and (c-I) event sequence phase-3 and a zoom (c-II).

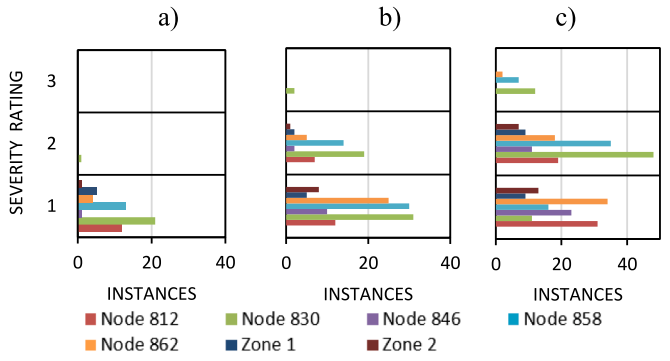

Fig. 9. Instances of different severity ranges (SR) at different measurement points for each event sequence phase during FADS implementation for capacitor bank switch malfunction. (a) Event sequence Phase-1, (b) event sequence Phase-2, (c) event sequence Phase-3.

somewhere between nodes 830 and 858, as they report most instances of level 2 and 3 SRs.

Phase-2 seems the ideal time to act in the FADS laboratory case study investigations. Mapping the Phase-2 timeline and implementing the FADS would help to detect the incipient failure a few weeks before the eventual equipment breakdown happens.

However, in this study case, the underperformance of the grid zoning concept is evident. The fallback option of LMD SRs must be used to locate the incipient failure accurately. Even though this case study highlights the need to implement optimization tools for better execution of the grid zoning concept, the overall FADS performance would not be affected much due to the inbuilt fail-safe feature of the two-tier SR system FADS tables should be numbered with Arabic numerals.

3.3. Transformer energization

The energization of a distribution transformer may generate overvoltage with high harmonic content and low damping due to the saturation characteristics of its iron core. This phenomenon is also characterized by inrush currents. Due to the habitual performance of connection and disconnection manoeuvres, it is one of the distribution systems' most common transitory processes. Transformer energization can cause a series of harmful effects both for the electrical system that feeds it and for the transformer itself, such as momentary voltage drops, temporary harmonic overvoltage, electromechanical stress on the windings, insulation deterioration, etc.

However, the transformer energization can cause troubles in the system. It cannot be considered an incipient fault but a programmed manoeuvre. Typically, the energization lasts 2 to 3 ms.

3.3.1. Experiment modeling

This document uses the IEEE-13 node feeder to evaluate the performance of the proposed method over a transformer energization. The transformer, which is connected is connected between 633 and 634, has the next characteristics. Transformer Y-Y Connection with Grounded Neutral, 4.16 kV to 0.48 kV, transformer rating 0.5 MVA leakage inductance 0.1 pu. The saturation is placed on the primary with 0.2 air core reactance values, knee voltage at 1.25 pu, 30 % loop width and 0.05 % of Eddy currents. At bus 634, only a 529 Ω shunt resistance is connected.

3.3.2. Simulation results

The simulation runs, complaining with previous simulations, for 260 s. There are no restrictions in transformer re-energization periods, but manufacturers suggest at least 12 hrs after a re-energization once the transformer is cold. Therefore, in this simulation, the sequence phases are related to the evolution of the event instead of an increase in the presence of distortions. In this way Phase 1 are the first 0.8 s, Phase 2 are from 0.8 s to 1.6 s and Phase 3 are from 1.6 to 2.4 s. Fig. 10 shows the phase A voltage waveforms for measurement at 633 and phase A at 634. The zoomed version of the voltage's waveform distortions is shown in Fig. 10 (a-II), and (b-II) to headline the transformer energization. It can be seen how the energization phenomena decrease the voltage at bus 633, and the nonlinearity produces several harmonics during the rest of the transient. Fig. 10 (b-II) shows similar behaviour. However, the voltage is zero at the beginning because the transformer is disconnected from the grid.

A summary of FADS results and instances of SR at different measurement points and zones is presented in Fig. 11. The same threshold obtained in Section 3.1 and Section 3.2 was used here. The energization is simulated at 0.04 s and does not occur after 12 hrs. Thus, in Phase-1, a few instances of level 1 SR are recorded. As expected, the measurement point next to the transformer records most instances. Only one recording

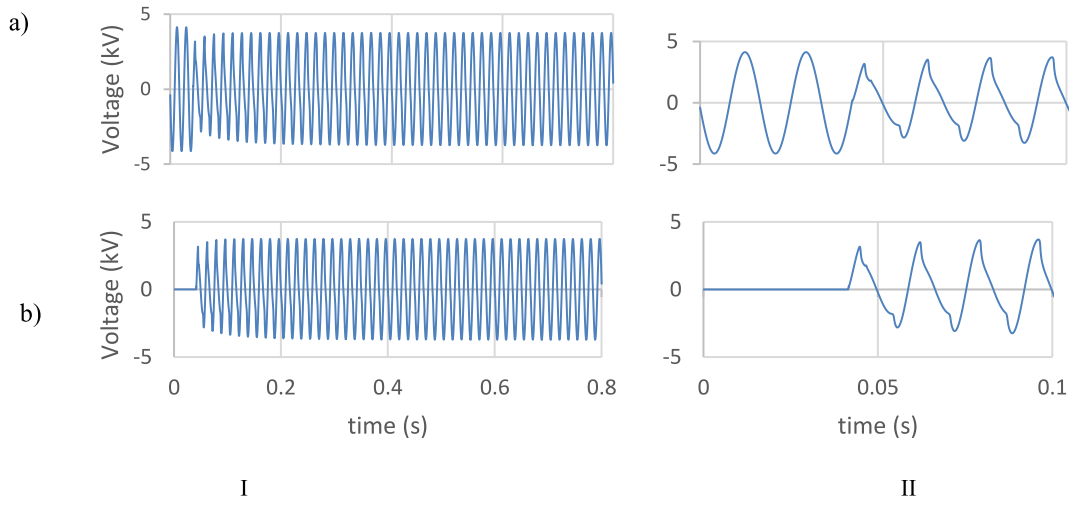

Fig. 10. Transformer energization event voltage waveform distortions event sequence phase 1 at buses (a-I) 633 phase A and (a-II) zoomed signal, (b-I) 634 phase A and a zoom (b-II).

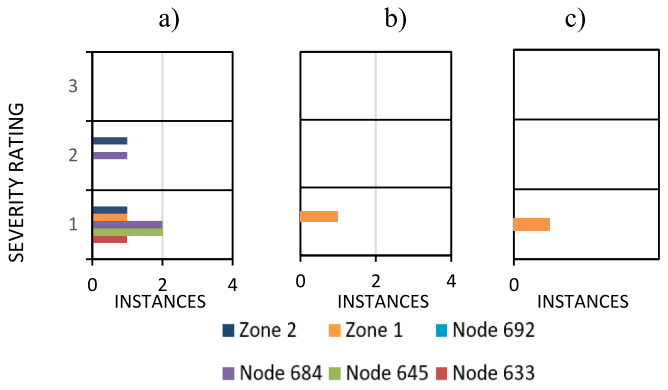

Fig. 11. Instances of different severity ranges (SR) at different measurement points for each event sequence phase during FADS implementation for transformer energization. (a) Event sequence Phase-1, (b) event sequence Phase-2 (after 0.8 s), (c) event sequence Phase-3(after 1.6 s).

point records a level 2 rating. The observations are inconclusive to confirm the presence of incipient failure. Fig. 11 (b) shows that after 0.8 s In Phase-2, the transformer energization transient tends to disappear, so there are only some instances in level 1. Phase-3, Fig. 11 (c) does not register any additional disturbance. The transient produced by transformer energization ends. It is worth saying that in this event, only the transformer energization was simulated as the only phenomenon. However, in real scenarios, the grid will face transformer energization and other switching operations. In an extreme scenario, the number of switching manoeuvres may lead to instances recorded in level 2 and could potentially fall in level 3 where the user may experience a false positive of an incipient fault, Zone 1 recordings are based on common reporting of nodes 633 and 634. While nodes 684 and 692 are used for Zone 2.

4. Conclusions

The paper proposes FADS as a comprehensive tool to anticipate incipient failures in power distribution systems. The majority of the failure anticipation methodologies, with the exception of [2,8], are restricted in their comprehensiveness by limited applicability; some are restricted by their comparatively high resource consumption and some by initial startup requirements. The work done in this paper takes a step forward and proposes an architecture and framework for a comprehensive and standardized failure anticipation and diagnosis scheme for power system protection. The FADS performance and speed anticipating the failure in the capacitor bank are similar to those observed in [14]. Leveraging the fundamental aspect of waveform distortions in complex exponentials leads to developing a robust yet low computational burden analysis technique for FADS. Severity scale and grid zoning concepts have been introduced in this paper for enhanced situational awareness and better planning of failure mitigation strategies.

Further improvements are needed in the context of implementation under real-field testing and performance optimization in different grid layouts and scenarios. However, FADS is flexible and user-friendly to adapt to real field complexities and regulations.

Declaration of competing interest

The authors declare that they have no known competing financial interests or personal relationships that could have appeared to influence the work reported in this paper.

Data availability

Data will be made available on request.

References

[1] Russell BD, Benner CL. Intelligent systems for improved reliability and failure diagnosis in distribution systems. IEEE Trans Smart Grid 2010;1(1):48–56. https://doi.org/10.1109/TSG.2010.2044898.
[2] Chang GW, Hong Y, Li G. A hybrid intelligent approach for classification of incipient faults in transmission network. IEEE Trans Power Delivery 2019;34(4):1785–94. https://doi.org/10.1109/PESGM41954.2020.9282041.
[3] IEEE Working Group on Power Quality Data Analytics, 2019, Tech. Rep. 73: Electrical signatures of power equipment failures. [online] Available: http://grouper.ieee.org/groups/td/pq/data/.
[4] Li B, Jing Y, Xu W. A generic waveform abnormality detection method for utility equipment condition monitoring. IEEE Trans Power Deliv 2017;32(1):162–71. https://doi.org/10.1109/TPWRS.2019.2904914.
[5] Samet H, Khaleghian S, Tajdinian M, Ghanbari T, Terzija V. A similarity-based framework for incipient fault detection in underground power cables. Int J Electr Power Energy Syst, 133;2021:107309, ISSN 0142-0615, https://doi.org/10.1016/j.ijepes.2021.107309.
[6] Kim CJ, Shin JH, Yoo M-H, Lee GW. A study on the characterization of the incipient failure behavior of insulators in power distribution line. IEEE Trans Power Deliv 1999;14(2):519–24. https://doi.org/10.1109/61.754097.
[7] Ghanbari T. Kalman filter based incipient fault detection method for underground cables. IET Gener Transm Distrib 2015;9(14):1988–97. https://doi.org/10.1049/iet-gtd.2015.0040.

[8] Gao B, Torquato R, Xu W, Freitas W. Waveform-based method for fast and accurate identification of subsynchronous resonance events. IEEE Trans Power Syst 2019;34 (5):3626–36. https://doi.org/10.1109/TPWRS.2019.2904914.
[9] Borges FAS, Fernandes RAS, Silva IN, Silva CBS. Feature extraction and power quality disturbances classification using smart meters signals. IEEE Trans Ind Inf 2016;12(2):824–33. https://doi.org/10.1109/TII.2015.2486379.
[10] Mousavi MJ, Butler-Purry KL. Detecting incipient faults via numerical modeling and statistical change detection. IEEE Trans Power Delivery 2010;25(3):1275–83. https://doi.org/10.1109/TPWRD.2009.2037425.
[11] Jazebi S, De Leon F, Nelson A. Review of wildfire management techniques-Part I: Causes, prevention, detection, suppression, and data analytics, IEEE Transactions on Power Delivery. doi: 10.1109/TPWRD.2019.2930055.
[12] Kulkarni S, Lee D, Allen AJ, Santoso S, Short TA. Waveform characterization of animal contact, tree contact, and lightning induced faults. IEEE PES General Meeting, Providence, RI, 2010, pp. 1-7. doi: 10.1109/PES.2010.5590214.
[13] Benner C, Purry KB, Russell BD. Distribution Fault Anticipator, EPRI, Palo Alto, CA, USA, Tech. Rep. Rep. 1001879; 2001.
[14] Wischkaemper JA, Benner CL, Russell BD, Manivannan K. Application of waveform analytics for improved situational awareness of electric distribution feeders. IEEE Trans Smart Grid 2015;6(4):2041–9. https://doi.org/10.1109/TSG.2015.2406757.
[15] Bhandia R, Chavez JDJ, Cvetković M, Palensky P. High impedance fault detection using advanced distortion detection technique. IEEE Trans Power Deliv 2020;35 (6):2598–611. https://doi.org/10.1109/TPWRD.2020.2973829.
[16] Dashti R, Daisy M, Mirshekali H, Shaker HR, Aliabadi MH. A survey of fault prediction and location methods in electrical energy distribution networks. Measurement 2021;184. https://doi.org/10.1016/j.measurement.2021.109947. ISSN 0263-2241.
[17] IEEE 519-2014: 'IEEE Recommended Practice and Requirements for Harmonic Control in Electric Power Systems, PE/T&D - Transmission and Distribution'; 2014.
[18] Schweitzer engineering laboratories. "User Manual SEL-487E-PMU and Relay Current Differential and Voltage Protection"; 2016.
[19] Siemens "User Manuel Line Differential Protection with Distance Protection 7SD5 v 4.7"; 2016.
[20] Schneider KP, et al. Analytic considerations and design basis for the IEEE distribution test feeders. IEEE Trans Power Syst 2018;33(3):3181–8. https://doi.org/10.1109/TPWRS.2017.2760011.
[21] Heydt GT, Graf TJ. Distribution system reliability evaluation using enhanced samples in a monte carlo approach. IEEE Trans Power Syst 2010;25(4):2006–8. https://doi.org/10.1109/TPWRS.2010.2045929.
[22] Moghe R, Mousavi MJ, Stoupis J, McGowan J. Field investigation and analysis of incipient faults leading to a catastrophic failure in an underground distribution feeder. IEEE/PES Power Systems Conference and Exposition, Seattle, WA, 2009, pp. 1-6. doi: 10.1109/PSCE.2009.4840203.